

Biosorption of some pharmaceutical compounds from aqueous medium by *Luffa cylindrica* fibers: application of the linear form of the Redlich–Peterson isotherm equation

Amel Aloui^{a,b}, Nouzha Bouziane^a, Hacene Bendjefal^{b,c,*}, Yacine Bouhedja^c,
Abdenour Zertal^a

^aLaboratory of Innovative Techniques for the Environment Preservation, University of Mentouri Brothers – Constantine 1 25000, Algeria, emails: aloui10amel10@gmail.com/amelsaloui@yahoo.fr (A. Aloui), bznouzha@yahoo.fr (N. Bouziane), azertal@hotmail.com (A. Zertal)

^bLaboratory of Physical Chemistry and Biology of Materials, Higher Normal School of Technological Education – Skikda 21000, Algeria, email: drbendjefal@gmail.com

^cLaboratory of Water Treatment and Recovery of Industrial Waste, Annaba University, 23000 Algeria, email: yybouhadje@yahoo.com

Received 11 May 2020; Accepted 23 October 2020

ABSTRACT

This study is focused on the removal of dextropropoxyphene (DPP) and paracetamol (PAR) from aqueous solutions by sorption on a low-cost biosorbent such as *Luffa cylindrica* fibers, which was initially characterized using Fourier-transform infrared spectroscopy and scanning electron microscopy and X-ray diffraction techniques. *Luffa cylindrica* fibers specific surface area was determined using adsorption/desorption isotherms of the N₂ gas method. The sorption study was realized by the batch method with the effect of the biosorbent amount, initial concentration, medium pH, and batch temperature. The modeling of the sorption phenomenon was based on the mathematical approach of the modified equation of Redlich–Peterson isotherm proposed by Feng-Chin-Wu, in which the dimensionless form of this isotherm, corresponding to the optimal curve, allows us to evaluate the α parameter. The same value of α was obtained for both pharmaceutical compounds, in which the $b_{RP}C_e^\alpha$ values are 2 for DPP and 10 for PAR. The linear regression of the Redlich–Peterson isotherm equation was also confirmed by analysis of variance. The obtained outcomes show that the probability value (p -value) is less than 0.05, with correlation coefficients (R_{adj}^2) 0.9515 for DPP and 0.9283 for PAR. The kinetics modeling analysis indicates that the biosorption mechanism can confirm pseudo-second-order and intraparticle diffusion. The adsorption of DPP and PAR is characterized by spontaneous and exothermic characters, in which the molecules of the two pharmaceutical products have a random behavior on the *Luffa cylindrica* active sites.

Keywords: Removal; Novel approach of Feng-Chin-Wu; Dimensionless form; Intraparticle diffusivity; Analysis of variance

1. Introduction

In the last decade, the removal of chemical, biochemical, and biological pollutants (heavy metals, dyes, and

pharmaceutical products) from natural aquatic mediums has become a necessary operation to save the environment. The great dispersal of these hazards is related directly to the fast growth of the manufacturing activities in our

* Corresponding author.

cities [1,2]. Pharmaceutical pollution has become an inevitable environmental problem of emerging concern; some of these compounds are persistent and have incompletely degraded in sewage treatment stations [3–5] due to their resistance to biodegradation [6]. In addition, the presence of these products in aquatic media can produce serious damage to different microorganisms [7].

The consumption of pharmaceutical compounds is increasing each year in a dreadful way, which can pose a great menace to life on earth [8]. Humans and animals in different levels of digestive transformation emit these products [9]. Many of these pharmaceuticals undergo degradation in nature and are transformed into by-products resulting from direct/indirect photolysis or hydrolysis [10]. In another way, the physicochemical parameters and the mechanisms that serve for the best natural degradation are not controlled. Fortunately, some of them can be removed by adsorption techniques under random environmental conditions. However, many compounds persist in aqueous systems around the world [11]. The presence of these chemicals in surface water may be explained by the incomplete removal of these hazardous compounds during wastewater treatment processes [12]. Unfortunately, there is little research on the identification of by-products such as metabolites and products of transformation from pharmaceutical elimination and degradation that persist in all types of water [13,14].

Dextropropoxyphene (DPP) and paracetamol (PAR) drugs are considered among the widely consumed pharmaceutical products. However, the occurrence of these drugs in water sources with high amounts may become dangerous for health. Recent studies revealed that DPP has been detected at important concentrations in surface waters [15]. In the estuary water, Roberts and Thomas [15] found that the DPP at concentrations varied between 0.008 and 0.033 $\mu\text{g/L}$. In contrast, the measured data in the sediments are almost nonexistent, in particular, the studied molecule.

PAR is characterized by antipyretic and analgesic medicinal activities. In addition, it seems to inhibit cyclooxygenase (Co_{x_1} – Co_{x_2}) in the nervous system [15]. It is frequently found in wastewater at a concentration of 6 $\mu\text{g/L}$ at the inlet of various treatment plants [15]. Although the maximum concentration of PAR in surface waters is approximately 0.11 $\mu\text{g/L}$ [16], which is considered a highly degradable compound, its concentration in seawater is very high and can reach 250 $\mu\text{g/L}$ [17].

The protection of aquatic ecosystems and different water sources against pharmaceuticals and their transformation products with undesirable and toxic effects has become the subject of several research works [7–9,11–13,18]. The chemical [19–23], biological [24], electrochemical [25], and bio-electrochemical [26] methods have proved their limitation towards the treatment of wastewater. In contrast, the adsorption method remains the most preferred technique in comparison with the other processes [19] due to the short-term investment of both cost and land, and it is considered a simple and very efficient process for the elimination of toxic and harmful substances [27,28]. The most commonly used adsorbent for pharmaceutical removal is activated carbon, which can be found as granular or powdery black material [29]. This material is characterized by

high porosity, an important surface area, and it has a good capacity in the elimination of toxic pollutants in a short time, but it is too expensive [30]. The selection of a highly efficient adsorbent is primordial for a successful adsorption process, especially in pharmaceutical elimination. However, adsorption onto the surface of natural materials such as clays (kaolin, bentonite), fibers (sisal, jute, and luffa) and marine algae is among the most commonly used processes in pollutant elimination and is considered a reasonable, low-cost, and green method [31].

The aim of this work is to evaluate *Luffa cylindrica* (*L. cylindrica*) as a natural material for DPP and PAR adsorptive removal from aqueous media at different values of temperature and pH. The adsorption experiences were realized using. The modeling analysis of the batch adsorption system is typically exhibited by a graphical representation of the solid-phase vs. its residual amount in aqueous solution [32]. This application is generally based on choosing an empirical relationship between experimental data and relevant dimensionless parameters using regression techniques [33]. Linear regression has been widely employed with success to investigate the parameters of sorption isotherms [33]. Modeling of some adsorption systems by plotting the solid-phase amount against the concentration of residual liquid using the two and three parameters of Langmuir, Freundlich and Redlich–Peterson isotherms has shown some inaccuracies. The poor precision of these isotherms is due essentially to a poor linear fitting model. Thus, Feng-Chin-Wu proposed a novel linear exponential form of Redlich–Peterson by estimating the three parameters of the isotherms using the characteristic line obtained from the dimensionless form of the Redlich–Peterson equation [34].

In this work, we first studied the application of *L. cylindrica* for DPP and PAR removal from an aqueous medium in a batch system. Second, the correlation of our experimental results using a mathematical approach, which is based on the linear form of the Redlich–Peterson isotherm equation proposed by Feng, was performed. The exponential form has shown great efficiency for fitting the Redlich–Peterson isotherm to experimental data obtained from sorption processes compared with the logarithmic form. The latter is currently used by selecting a suitable range of α values, which was determined from the dimensionless form plot of the Redlich–Peterson equation. Analysis of variance was also employed to investigate the adequacy of the fitted model by determining the adjusted correlation coefficients (R_{adj}^2) and the mean sum of squares (SS). Statistical significance is judged by the Fisher value and the probability value, which must be less than 0.05 [35].

Note that our group is the first to perform this kind of research study, which was dedicated to elucidate the adsorptive properties of *L. cylindrica* for the removal of pharmaceutical products from water.

2. Materials and methodology

2.1. Reagents

The biosorbent *L. cylindrica* was purchased from a local shop in Skikda, Algeria, in which only *L. cylindrica* fibers were used. The adsorption experiments were carried out with two pharmaceutical products, dextropropoxyphene

(Sigma-Aldrich, United States, 98.22%) and paracetamol (Merck, Germany, 99.6%), in which the chemical reagents were used with analytical grade and deionized and distilled water were used throughout this study. The main physico-chemical properties of those products are collected in Table S1.

2.2. Adsorbent pre-treatment and characterization

100 g of luffa fibers were soaked in 1 L of hydrogen peroxide for 2 d to remove adhering dirt. Thereafter, the *L. cylindrica* fibers were rinsed for 3 h using distilled water and then dried at 80°C for 12 h. Then, they were dipped in NaOH (0.1N) solution for 1 h to increase their hydrophilicity. The obtained alkalinized fibers were finally cleaned with distilled water and dried again at 80°C for 12 h.

The Fourier-transform infrared spectroscopy (FTIR) spectrum of the treated fibers was obtained using a Shimadzu Spectrometer (FTIR 8700, Japan) with the KBr pellet method. The spectra were registered in a spectral range from 400 to 4,000 cm^{-1} with a resolution of 4 cm^{-1} . The surface morphology of the treated fibers was also analyzed using scanning electron microscopy (SEM) (JEOL, JSM-7600F, Japan). Additionally, the porosity of those fibers was studied using adsorption/desorption isotherms of nitrogen gas measured at 77 K using Cooltronic Micromeritics 2100E model surface area analyzer (China). The specific surface area of *L. cylindrica* was calculated using the Brunauer–Emmett–Teller (BET) equation.

2.3. pH of zero point charge (pH_{pzc})

The determination of pH_{pzc} was realized to establish the pH value in which the *L. cylindrica* surface net charges are zero. To do this, 100 mg of *L. cylindrica* fibers was added to 50 mL of aqueous solution, in which the initial pH was adjusted with HCl or NaOH solutions in the range of 2–12. The mixture was stirred at room temperature for 24 h, and then the pH was measured. The zero point charge is reached where the final pH does not change after contact with the *L. cylindrica* fibers.

2.4. Biosorption experiments

The adsorption of DPP and PAR on *L. cylindrica* fibers was performed on single component in batch system. DPP and PAR stock solutions of 200 mg/L were prepared separately by dissolving of 50 mg of each pharmaceutical compound in 250 mL of deionized water, which were further diluted to obtain the desired concentrations for the study (20–120 mg/L). The adsorption experiments were carried out at varying adsorbent dose, medium pH, adsorptive initial concentration, and temperature to determine an optimum set of conditions for maximum adsorption. 100 mL of aqueous drug solution was placed in a glass cylindrical flask and it was mixed with 100 mg of *L. cylindrica* fibers, at a particular pH and constant temperature. After shaking for 60 min of contact, the suspension was filtered through the Whatman filter. The DPP and PAR residual concentrations were determined using a Shimadzu UV-Vis spectrophotometer at a maximum wavelength of 257 and 243 nm, respectively.

2.5. Effect of physicochemical factors on the adsorption processes

Optimization of the operating conditions was performed by varying one parameter and setting the other constants. Thus, for the pH effects at room temperature, a mixture containing 0.1 g of luffa fibers and 50 mg/L of a solution of each pharmaceutical is subject to a variation in pH between 2 and 12. To study the temperature effects under the original value of solution pH, the same quantities of reagents were taken by varying the temperature in the range between 10°C and 50°C. Finally, for the optimal luffa mass, this parameter was obtained by changing the mass of luffa fibers from 0.05 to 0.4 g under the following experimental conditions: 50 mg/L of solution, original pH, and room temperature.

The removal efficiencies (R%) of DPP and PAR were determined under various experimental conditions according to the following equation:

$$R\% = \frac{(C_0 - C_t)}{C_0} 100 \quad (1)$$

where C_0 and C_t are the concentration (mg/L) of adsorptive at the initial and t times, respectively. The adsorption amount (q_e) of DPP and PAR was estimated within the following formula:

$$q_e = \frac{(C_0 - C_e)}{W} V \quad (2)$$

where C_e is the DPP and PAR equilibrium concentration (mg/L) in aqueous media, W is the weight of the biosorbent (g) and V is the solution volume (L).

2.6. Adsorption isotherms

Previous studies indicate that the Redlich–Peterson (RP) isotherm model is more accurate than the Freundlich and Langmuir equations in describing adsorption systems [34,36]. The RP isotherm equation is mainly used to explain the formation of the monolayer with multi-site interaction phenomena at the same time [37]. The three parameters of the Redlich–Peterson and Sips isotherm models are employed to study both homogeneous and heterogeneous adsorption systems [38]. In addition, the RP isotherm integrates the isotherms of Freundlich and Langmuir into a single equation [39]. The nonlinear Redlich–Peterson isotherm equation is given by:

$$q_e = \frac{q_{\text{mon}} b_{\text{RP}}}{1 + b_{\text{RP}} C_e^\alpha} C_e \quad (3)$$

where b_{RP} and q_{mon} are the parameters of the Redlich–Peterson isotherm equation. The value of the exponent, α , is in the range from 0 to 1 because it has two limiting behaviours: Henry's law form for α equal to 0 and Langmuir form for α equal to 1. At low concentrations, it is also comparable to the Henry isotherm and performs the Freundlich equation for high concentrations [40]. The linear and non-logarithmic form of Eq. (3) is given by Eq. (4).

$$\frac{C_e}{q_e} = \frac{1}{b_{RP}q_{mon}} + \left(\frac{1}{q_{mon}} \right) C_e^\alpha \quad (4)$$

The dimensionless form of the RP equation proposed by Feng-Chin-Wu is expressed as follows:

$$\frac{q_e}{q_{ref}} = \left(\frac{C_e}{C_{ref}} \right) \frac{\left(\frac{1}{b_{RP}C_e^\alpha} \right) + 1}{\left(\frac{1}{b_{RP}C_e^\alpha} \right) + \left(\frac{C_e}{C_{ref}} \right)^\alpha} \quad (5)$$

Here, C_{ref} is the highest equilibrium concentration of the adsorption system, and q_{ref} is the equilibrium adsorption quantity at C_{ref} . α is a parameter attained by trial and error for $b_{RP}C_{ref}^\alpha = 2$ and 10, respectively [34], in which its value must be less than 1. The plot of q_e/q_{ref} vs. C_e/C_{ref} of Eq. (5) gives an indication of the optimal line that corresponds to the appropriate α value. The data obtained from the batch concentration studies were fit into the Redlich–Peterson expression. The linear regression lines have been realized by plotting C_e/q_e vs. the C_e^α of Eq. (4), using different values of α . The values of C_e^α were calculated for each α value in the first place, and then, the regression line associated with the specific value was plotted. The values of the other factors, such as b_{RP} and q_{mon} , have been estimated from the intercept and slope of the linear plot of Eq. (4). Analysis of variance was performed to confirm the validity of the mathematical model. This analysis is based on the presentation of the statistical results and the diagnostic checking test, which allows us to evaluate the mathematical model [41]. Thus, if the p -value is less than 0.05, the studied model is significant. The low mean square SS also indicates that the model is the best.

3. Results and discussion

3.1. Characterization of the biomaterial

The fibers of *L. cylindrica* are composed of 60% cellulose, hemicelluloses 30% and 10% lignin, which makes it a flexible and durable biosorbent [42]. Analysis of *L. cylindrica* using SEM shows the presence of macropores in the structure of the *L. cylindrica* fiber (Fig. 1). From Fig. 1, we can notice the fibrous nature with some fissures and small holes of about 1 μm in diameter, which may facilitate the biosorption of DPP and PAR. The specific surface area (S_{BET}) and porosity are considered important factors for evaluating the adsorptive capacity of solid materials. The S_{BET} of *L. cylindrica* fibers was investigated using the N_2 adsorption and desorption isotherm, as shown in Fig. 2. It can be seen that the N_2 adsorption/desorption isotherm curves belong to the type (III) isotherm; in such cases, the adsorbent–adsorbate interaction is weak compared with the adsorbate–adsorbate interactions [43]. The adsorbed molecules are clustered around the most favourable sites on the surface of a nonporous or macroporous solid. The form of hysteresis was attributed to adsorption metastability. In an open-ended pore (e.g., of cylindrical geometry), the metastability comes from the delayed condensation of the adsorbed multilayer. It follows that in an assembly of such pores, the adsorption branch of the hysteresis loop is not in thermodynamic equilibrium. Therefore, if the pores are filled with liquid-like particles, thermodynamic equilibrium is established on the desorption branch [44]. The dv/dD against pore size curve illustrates that the higher pore size is about 50 nm, which confirmed the macroporous form of sorbent [43]. The surface area of *L. cylindrica* fibers was determined to be 123 m^2/g .

The pH_{pzc} of the *L. cylindrica* fibers and that of the modified *L. cylindrica* fibers is 5.59 and 8.60, respectively

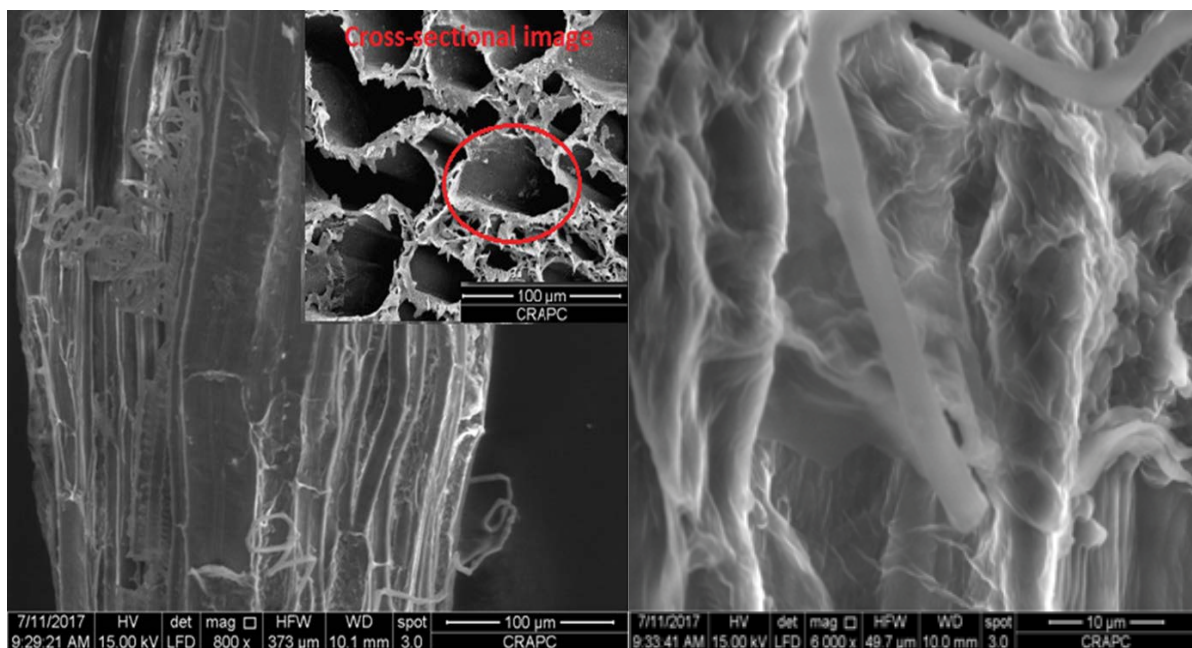


Fig. 1. Scanning electron microscopy of *Luffa cylindrica* fibers (cross-sectional image of macropores).

(Fig. 3). This difference may be attributed to the effects of the alkaline treatment. Therefore, the surface of the modified *L. cylindrica* is predominantly positively charged if the pH is lower than 8.60 and negatively charged if it is higher than this value. As a consequence, the adsorption of pharmaceutical compounds may depend on the change in pH.

The FTIR spectrum of the alkalinized *L. cylindrica* is illustrated in Fig. 4, together with the wavenumbers of significant bands associated with the functional groups of the alkalinized *L. cylindrica* surface. The spectrum displays a strong band located at 3,445 cm^{-1} , indicating the presence of O–H groups. The bands situated between 2,858 and 2,920 cm^{-1} are attributed to the absorption of symmetrical vibration in the C–H bond. The peak appeared at about 1,763 cm^{-1} is assigned to the C=O bond (pectin) [45]. The small band at 1,389 cm^{-1} corresponds to the C–H bond, and the shaper band at 1,404 cm^{-1} corresponds to CH_2 and CH_3 groups. The band located at 1,516 cm^{-1} is due to the stretching vibration of the C=C of the benzene ring (lignin) [30]. The peaks ranging between 1,000 and 1,300 cm^{-1} correspond to the absorption of C=O (ketones), especially the

clear peak close to 1,059 cm^{-1} representing C–O (cellulose) [45]. The peaks observed at 1,177 cm^{-1} may correspond to the C–O–C of cellulose and hemicelluloses [30]. Finally, the absorption of the C–C bond is attributed to the presence of the peaks located between 814 and 941 cm^{-1} .

The determination of the crystal structure and atomic spacing of an adsorbent is considered an important parameter usually used to study sorption phenomena, which can be realized using the X-ray diffraction (XRD) technique [46–49]. Fig. 5 shows the XRD diffractogram of the used *L. cylindrica* fibers. We can clearly see that the *L. cylindrica* fibers have an amorphous structure, which can be explained by the presence of noncellulosic compounds in the *L. cylindrica* structure. Indeed, the broad peaks located at 16.8° and 22.9° are attributed to the indexed planes (100) and (200), respectively, corresponding to the presence of cellulose compounds (ICDD card N°. 00-003-0226) in the structure of the used *L. cylindrica* fibers [47–49].

3.2. Parameters affecting the DPP and PAR adsorption process

3.2.1. Effect of the medium pH

The adsorptive removal of organic and inorganic pollutants can be significantly affected by the initial pH of the aqueous medium. Indeed, the concentration of hydroxyl and hydrogen ions affects the adsorption process through the dissociation of the functional groups on the adsorbent surface and/or the ionization of the adsorbed molecules [30]. The variations in DPP and PAR removal by *L. cylindrica* at various pH values (from 2.0 to 12.0) are depicted in Fig. 6a.

An analysis of Fig. 6a reveals that under all experimental pH values, except pH 10, the adsorption process is more efficient with PAR than DPP. Moreover, the percentage of removal seems to exhibit different behaviours. The structure of luffa indicates the presence of hydroxyl groups (–OH) and taking into account the presence of nitrogen N atoms in the structure of PAR, which has a non-bonding electron pair, the retention on the surface of *L. cylindrica* may be achieved mainly by hydrogen bonds (particular type of physical interactions). On the other hand, the presence

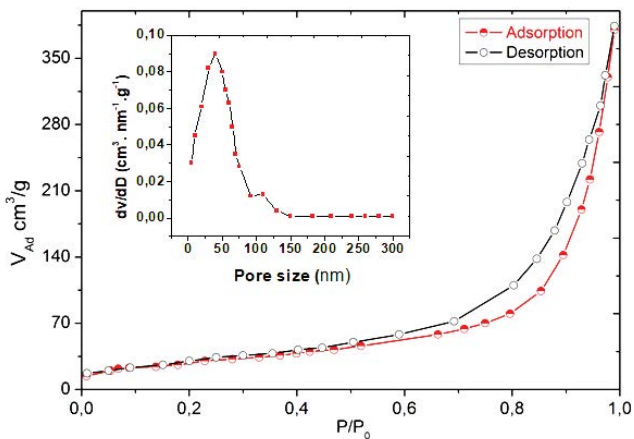


Fig. 2. N_2 adsorption/desorption isotherms and pore size distribution analyses of *Luffa cylindrica* fibers.

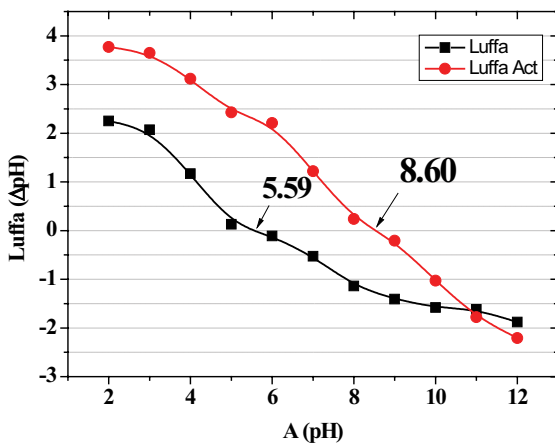


Fig. 3. pH of zero charges of natural and modified *Luffa cylindrica*.

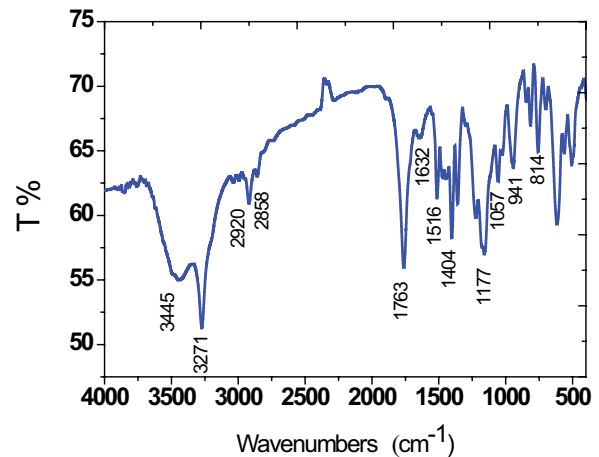


Fig. 4. Fourier-transform infrared spectrum of alkalinized *Luffa cylindrica* biosorbent.

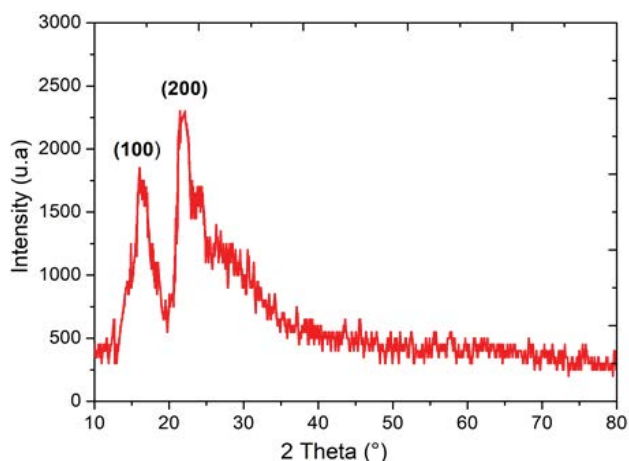


Fig. 5. X-ray diffractogram of the *Luffa cylindrica* fibers.

of the benzene ring in the adsorptive structure as well as the adsorbent may lead to the creation of other physical electrostatic interactions, such as van der Waals forces.

In the reaction of PAR with a strong acid, such as HCl, which has been used in this study, PAR reacts as a proton acceptor. According to the structure of PAR, there are two possibilities of site protonation: the OH group and the amide function. However, the addition of HCl does not react with the OH group because the oxygen loses its non-bonding electron pair by conjugation, and thereby it reacts only with the oxygen atom of the amide function that does not participate in the conjugated system of PAR. Therefore, in the pH range between 2 and 7, there is no effect. Protonation on the adsorption efficiency occurs because the OH group of PAR stays free and can participate by hydrogen bond interactions with luffa fibers.

The acidity of phenols is admittedly low but not negligible ($pK_a = 9.5$); therefore, the addition of a strong base such as NaOH will lead to the deprotonation of the hydroxyl group (phenolic OH). Deprotonation may be partial if the medium is weakly alkaline due to an insufficient amount of NaOH for deprotonation of PAR. In contrast, the deprotonation becomes increasingly pronounced with increasing pH, leading to the formation of a phenoxide anion. The amide function remains unchanged at low pH values (up to 10). A decrease in the sorption efficiency at lower pH was observed (Fig. 6a) indicates the possibility of repulsion between the *L. cylindrica* fibers surface charged positively as well as the carbocation of PAR and the formation of PAR dimers in the solution. As adsorption efficiency decreases with decreasing solution pH, it can be confirmed that the donor-acceptor electron mechanism is weakly active in this sorption [50]. It is the same for DPP. An increase in the solution pH enhances the adsorption and reaches a maximum at pH = 10.0 for both pharmaceuticals (PAR and DPP). This can be attributed to the electrostatic repulsion between adsorptive molecules and the *L. cylindrica* surface, which is created from the negative charge that each carries. At pH = 12, PAR ($pK_a = 9.5$) and DPP ($pK_a = 6.3$) were present in their dissociated anionic form, and the surface of alkaline *L. cylindrica* was negatively charged. Hence, repulsion phenomena are predominant and

determine the observed reduction in adsorption efficiency (Fig. 6a). In conclusion, the obtained results in the present study determined that the adsorption efficiency is highest at pH = 10.0 for both compounds, at which $R = 83.13\%$ and 67.97% for PAR and DPP, respectively. At pH = 12.0, the adsorption efficiency decreased to 65% for PAR and 62.26% for DPP.

3.2.2. Effect of *L. cylindrica* mass

The effect of *L. cylindrica* mass on the removal of DPP and PAR from aqueous was carried out using adsorbents dose in the range of 0.05–0.4 g, while the other parameters such as contact time, medium pH, and temperature were kept constant. Fig. 6b shows that the use of 0.1 g of *L. cylindrica* was sufficient to eliminate 53.52% of DPP and 95.55% of PAR.

Therefore, this amount allows fixing the greater part of each pharmaceutical molecule on sorbent sites. From Fig. 6b, we can notice that the removal efficiency increases with increasing *L. cylindrica* fibers dose until a certain level, whereabouts all active sites for the sorption of pharmaceutical compounds are available [51]. Thus, beyond a dose of 0.1 g, there is no considerable change in the adsorption amount [52]. Such a phenomenon is caused by a large amount of adsorbent that may reduce the instauration of the adsorption sites and/or create particle aggregation, leading to a reduction in the total surface area and an increase in diffusion path length, which contribute to a decrease in the adsorbed amount [51–53].

3.2.3. Effect of pharmaceutical initial concentration

Regarding the initial concentration for each pharmaceutical, the highest rate of DPP adsorption (54.29%) is attributed to a 50 mg/L concentration (Fig. 6c). The optimal initial concentration of PAR, corresponding to the highest elimination rate ($R = 70.70\%$), is 20 mg/L. However, at initial concentrations of DPP and PAR higher than 20 and 50 mg/L, respectively, the removal efficiencies were slightly decreased, which may be due to the saturation in adsorptive sites on the surface of *L. cylindrica* fibers and to the occupation of the less energetically favoured sites with increasing DPP and PAR concentrations in solution [51–53].

3.2.4. Effect of media temperature

The temperature is considered as an important parameter to study the adsorption of pharmaceutical compounds; their effect is very useful in the determination of thermodynamic parameters allowing the characterization of the adsorption processes. However, in the case of the adsorption of DPP and PAR onto *L. cylindrica* fibers, it seems that the temperature has an insignificant effect on the adsorption process, with a removal efficiency ranged between 46.74% and 56.31% in the case of DPP and between 94.36% and 95.27% for PAR as shown in Fig. 6d.

3.3. Adsorption isotherms

The obtained results from the application of the new mathematical approach of RP isotherm equations are listed in Table 1 and illustrated in Fig. 7. Figs. 7a and c represent

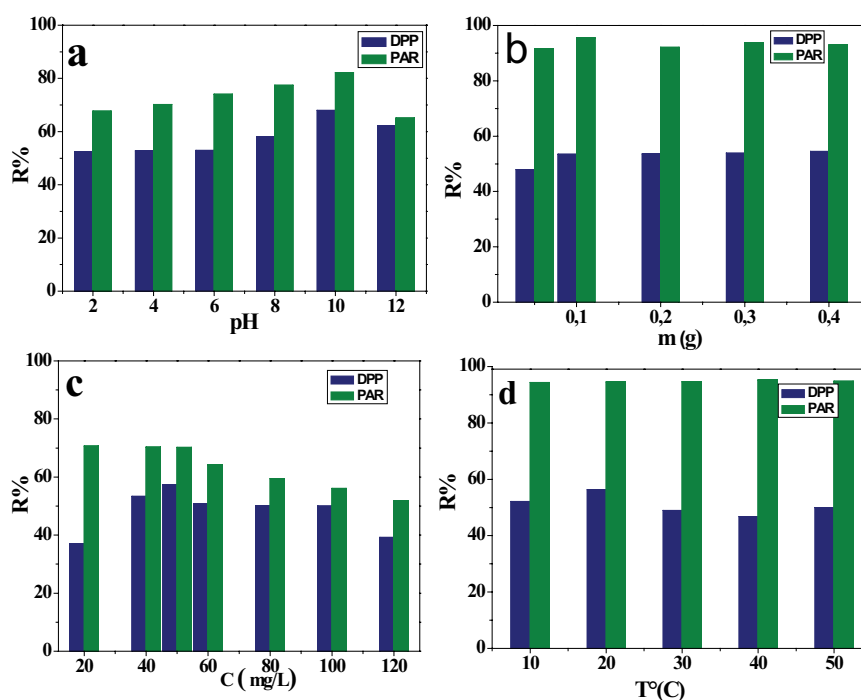


Fig. 6. Histogram of different parameters affecting dextropropoxyphene and paracetamol biosorption onto *Luffa cylindrica* fibers.

the dimensionless RP form obtained by Eq. (5). These figures illustrate the presence of a single line that passes through the experimental points, in which α value is less than unity, verifying the main condition of the RP theorem. This line corresponds to an α value equal to 0.8 in the cases of DPP and PAR. Nevertheless, with the difference in the $b_{RP}C_e^\alpha$ value, in which $b_{RP}C_e^\alpha$ is 2 for DPP and 10 for PAR, the data of DPP and PAR adsorption have been investigated according to the linear form of the Langmuir isotherm of Eq. (3), in which α is equal to unity.

The obtained results are collected in Table 2, where b_{RP} has become K_L and q_{mon} is taken as q_m . These lines are linear over the majority of the experimental points on the studied concentration range for DPP and PAR, with an extremely high value of R_{adj}^2 for PAR ($R_{adj}^2 = 0.9364$). Tables 1 and 2 show that the biosorption model constants of DPP onto *L. cylindrica* fibers are well defined by the RP equation since a higher adjusted linear regression correlation coefficient was obtained for this model (0.95). On the other hand, the constant of the PAR adsorption isotherm onto *L. cylindrica* was found to be equal to 0.93 for the Langmuir model, which was obtained using the linear equation RP when α was equal to 1 (Table 2). The high value of monolayer sorption capacity for PAR ($q_m = 97.0873$ mg/g) indicates that *L. cylindrica* fibers have homogeneous surface energy [54].

Analysis of variance was performed to test the goodness of the studied model fit. Thus, the model data forms are significant if the SS or mean square are obtained with small values, in which the p -value should be less than 5% and the F -value will be higher than this value. From an analysis of data in Table S2, we can conclude that the regression explains well the studied phenomenon since the meaning of the model risk is less than 0.05 ($p < 1.8411 \times 10^{-5}$ for PAR and $p < 5.7114 \times 10^{-4}$ for DPP). For evaluation of the obtained

Table 1
Parameters of the Redlich–Peterson isotherm

	α	q_{mon} (mg/g)	b_{RP}	R_{adj}^2
Dextropropoxyphene	0.8	33.8066	0.5898	0.9515
Paracetamol	0.8	38.2895	3.4355	0.9265

model, the calculations of the F -value (99.1702 for DPP and 104.6546 for PAR) confirm that this model is extremely significant. Thus, the adequacy of the fitted model has been judged by the adjusted coefficient of correlation R_{adj}^2 that is the correlation between the experimental and adapted model, which measures the total variation proportion in the average response clarified by the regression. Furthermore, this coefficient is sufficient to give a concordance between the experimental results and the adapted model of the linear exponential form of the RP isotherm (Eq. (4)). Figs. 7b and d show the goodness of fitting the experimental results. Thus, the value of R_{adj}^2 (Table 1) indicates that only 4.85% and 7.45% of the total variation of DPP and PAR, respectively, which not could be explained by the adapted model.

3.4. Adsorption kinetic modelling

The nature of the adsorption process depends essentially on the physicochemical properties of the used adsorbent surface and the nature of the adsorbent. To study the mechanism and rate of DPP and PAR biosorption processes onto *L. cylindrica* fibers, the obtained kinetic outcomes of DPP and PAR adsorption were correlated using various conventional methods, namely, intraparticle diffusion, pseudo-first, and pseudo-second-order kinetic methods.

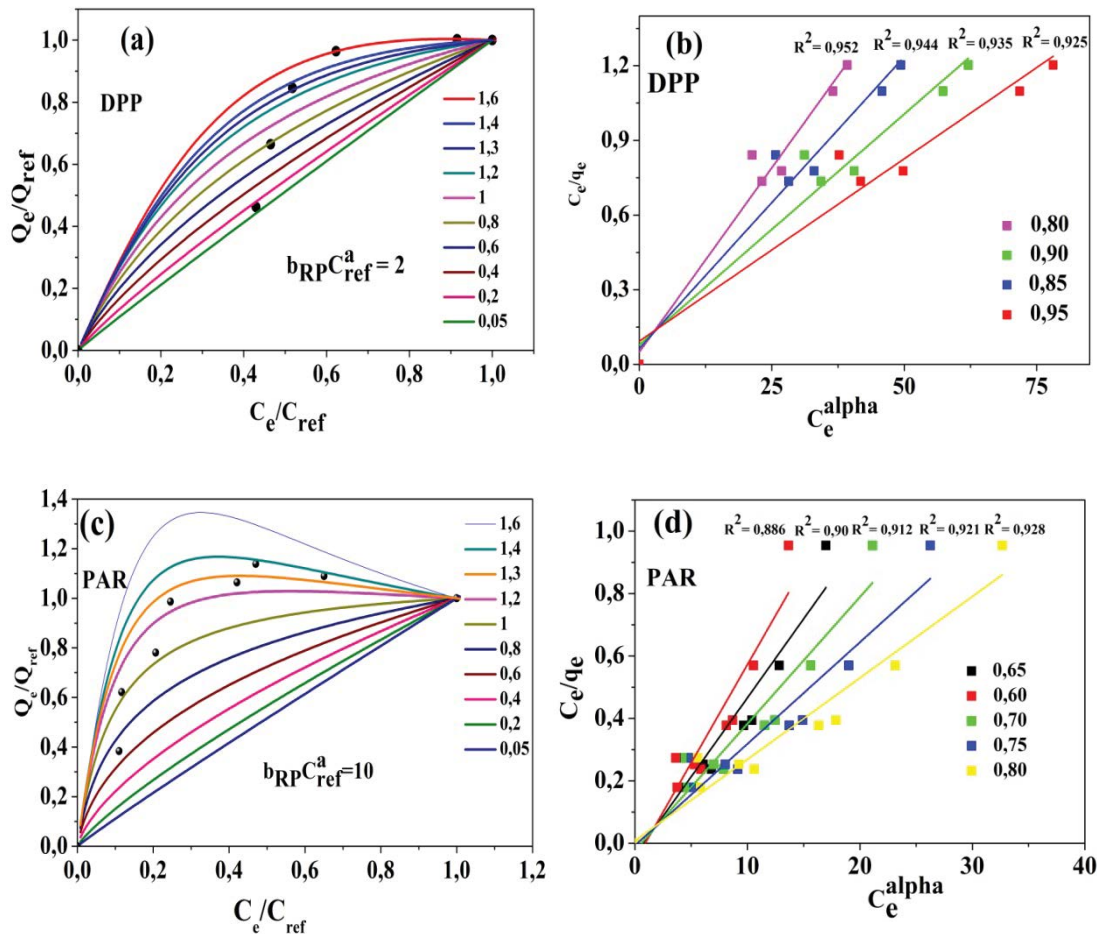


Fig. 7. Dimensionless Redlich–Peterson form (a and c) and exponential linear form of Redlich–Peterson (b and d) of dextropropoxyphene and paracetamol.

Table 2

Parameters and analysis of variance for adsorption of dextropropoxyphene and paracetamol for $\alpha = 1$ (Langmuir isotherm resulting from Redlich–Peterson model)

	K_L	q_m (mg/g)	R^2_{adj}	Sum of squares	F-value	p-value
Dextropropoxyphene	4.4305	12.1951	0.8320	0.1499	20.8048	0.010
Paracetamol	7.7864	97.0873	0.9364	0.4246	104.0418	5.1727×10^{-5}

Table 3 collects the principal experimental adsorption data obtained using DPP and PAR initial concentrations of 40 and 60 mg/L, respectively, and 0.1 g of adsorbent in 100 mL of distilled water. Lagergren [55] proposed the kinetic model of pseudo-first-order using an empirical equation (Table 3), which plots $\ln(q_e - q_t)$ in terms of the contact time. Several previous studies indicated that this equation is a fruitful model in which it can provide a good linear relationship between k_1 and q_e , which may be confirmed from its slope and interception.

An analysis of the experimental q_e values shows that, the distance of the interception is aptness and failed to describe the experimental outcomes. In addition, the adsorption rate does not obey this equation. On the other hand, the adsorption kinetics are explained using the

pseudo-second-order kinetic model [56]. Thus, this last produces a straight line and high values of R^2 . The adsorption equilibrium capacity (q_e) and k_2 were extracted from the intercept and the slope curve and from the plot of t/q_t vs. t , respectively. The predicted capacity of adsorption (q_e), the correlation coefficient values (R^2) and the experimental closeness values demonstrate that the second-order model successfully explains our experimental data (Table 3). The correlation coefficient (R^2) values reached 0.9999 and a great similarity between the calculated values of adsorption equilibrium capacity (q_e) and that of the experimental adsorption capacity was obtained under different experimental conditions. Moreover, the process has also been studied using the intraparticle diffusion model [57]. This model is based on liquid film mass transfer diffusion, in

Table 3
Kinetic model rate parameters obtained using the linear equations

Model	Equation	Parameter	Value of parameters			
			40 mg/L		60 mg/L	
			Dextropropoxyphene	Paracetamol	Dextropropoxyphene	Paracetamol
First-order kinetic	$\ln(q_e - q_t) = \ln(q_e) - k_1 t$	k_1	0.1274	0.2477	0.1432	–
		$q_{e,cal}$	1.6538	0.7422	2.8352	–
		R^2	0.7622	0.8307	0.9687	–
Second-order kinetic	$\frac{t}{q_t} = \frac{1}{k_2 q_e^2} + \frac{1}{q_e} t$	k_2	0.3329	2.1595	0.1743	2.2050
		$q_{e,cal}$	36.1402	39.2157	54.945	59.1366
		R^2	0.9999	0.9999	0.9999	0.9999
Intraparticle diffusion	$q_t = K_{dif} t^{1/2} + C$	K_{dif}	0.1584	0.8442	0.1403	0.8442
		C	36.1879	37.2284	53.8869	57.2289
		R^2	0.9190	0.9251	0.8974	0.9251
		$q_{e,exp}$	36.0909	39.1414	54.7273	59.0995

which the sorption rate is related to the square root ($t^{1/2}$). The K_{dif} and C values were determined from the slope and intercept of the q_t vs. $t^{1/2}$ plot, respectively.

The values of C that are related to the boundary layer thickness and the rate constant intraparticle diffusion K_{dif} are collected in Table 3. Since the curve of the intraparticle diffusion model does not pass through the origin (Fig. 8), this indicative of some degree of boundary layer control and this further shows that the intraparticle diffusivity is not the only rate-controlling step; but also other processes may control the rate of adsorption [54,58].

3.5. Thermodynamic study

The values of the thermodynamic parameters of DPP and PAR sorption, namely, the relative Gibbs free energy (ΔG°), relative enthalpy (ΔH°) and relative entropy (ΔS°), were calculated using the following equations:

$$\Delta G^\circ = -RT \ln K_d \tag{6}$$

$$\ln K_d = \frac{\Delta S^\circ}{R} - \frac{\Delta H^\circ}{RT} \tag{7}$$

where K_d is the thermodynamic equilibrium constant, R is the gas universal constant, and T is the absolute temperature (in Kelvin).

The obtained results of the thermodynamic study are collected in Table 4 and illustrated in Fig. S1. From Table 4, we can notice that all relative Gibbs free energy values have negative values, which account for a spontaneous and feasible process. In addition, the ΔG° values decreased with increases in temperature. On the other hand, the negative values of ΔH° indicate that the studied sorption process has an exothermic character, which may be attributed to a physical mechanism [59], characterizing the adsorption of DPP and PAR. At the same time, the negative values of ΔS° account for a decrease in the concentration of DPP and PAR in the solid–liquid interface, thereby indicating that there is an increase in the concentration of DPP and PAR on the surface of the solid phase.

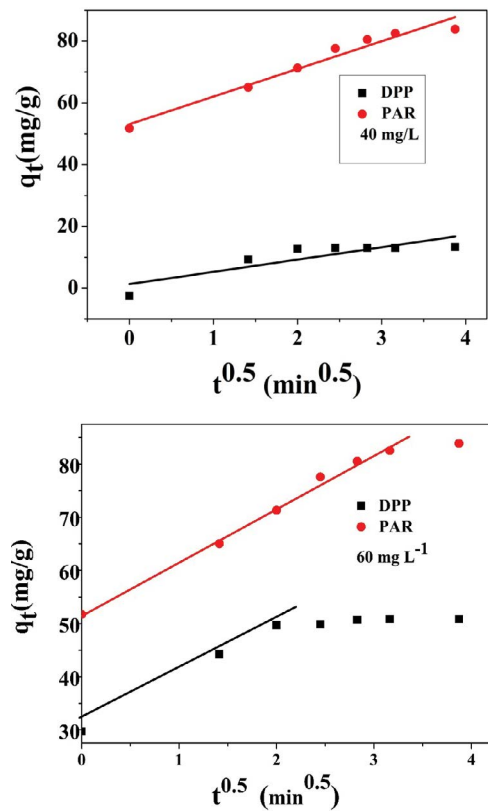


Fig. 8. An intraparticle diffusion model for dextropropoxyphene and paracetamol adsorption on luffa fiber at different initial concentrations (40 and 60 mg/L).

4. Conclusion

In this work, we have performed an experimental study for the goal of removing DPP and paracetamol (PAR) from aqueous solutions by sorption on a low-cost biosorbent such as *L. cylindrica* fibers, as well as modeling the sorption phenomenon based on the mathematical approach of the modified equation of the Redlich–Peterson (RP)

Table 4
Thermodynamic parameters for biosorption of dextropropoxyphene and paracetamol onto *Luffa cylindrica*

	Parameters	Temperature (K)				
		283	293	303	313	323
Dextropropoxyphene	ΔG° , (kJ/mol)	-10.9023	-12.8189	-17.5344	-20.4570	-27.9211
	ΔH° , (kJ/mol)			-12.9798		
	ΔS° , (J/mol K)			-54.9405		
Paracetamol	ΔG° , (kJ/mol)	-821.2689	-178.6351	-1,265.7614	-136.2763	-196.9254
	ΔH° , (kJ/mol)			-5.4453		
	ΔS° , (J/mol K)			-16.7427		

isotherm. The main conclusions extracted from the obtained outcomes are as follows:

- This study demonstrates the suitability and applicability of the novel dimensionless and exponential linear forms of the RP isotherm proposed by Feng-Chin-Wu, which allowed us to easily determine the parameters of the RP model for DPP and PAR.
- The α value was equal to 0.8 for each studied pharmaceutical compound, corresponding to an optimum line that gives the other parameters, mainly b_{RP} and q_{mon} .
- The RP equation involving adsorption on homogeneous active sites is definitely the most suitable modeling tool to satisfactorily describe DPP biosorption. The Langmuir model showed great adequacy in describing the adsorption experimental data of PAR onto *L. cylindrica* by providing the highest adjusted squared correlation coefficient R^2 and the lowest p -value.
- The kinetics curves are characterized by the pseudo-second-order rate equation, in which the intraparticle diffusion was not the only rate-determining step.
- The thermodynamic study shows that the obtained parameters confirmed that the adsorption process is exothermic and spontaneous and that the molecules of the studied drugs have random behavior on the surface of the *L. cylindrica* fibers.

Declarations

Funding: Not applicable

Acknowledgments

The authors thank Prof Khorief Nacer Eddine Abdelmalek (Laboratory of Physical Chemistry and Biology of Materials, Higher Normal School of Technological Education–Skikda 21000, Algeria) for his time to check and polish the language of this paper.

Competing interests

The authors declare that they have no competing interests.

Authors' contributions

The manuscript was prepared by A. Aloui and written through the contributions of all authors. All authors read and approved the final version of this manuscript.

References

- [1] M.E. Matsubara, K. Helwig, C. Hunter, J. Roberts, E.L. Subtil, L.H.G. Coelho, Amoxicillin removal by pre-denitrification membrane bioreactor (A/O-MBR): performance evaluation, degradation by-products, and antibiotic resistant bacteria, *Ecotoxicol. Environ. Saf.*, 192 (2020) 110258, <https://doi.org/10.1016/j.ecoenv.2020.110258>.
- [2] Y.S. Ji, X.L. Zhang, J.T. Gao, S.J. Zhao, Y.K. Dou, Y. Xue, L.H. Chen, Efficiency and mechanisms of cadmium removal via core-shell zeolite/Zn-layer double hydroxides, *Ecotoxicol. Environ. Saf.*, 188 (2020) 109887, <https://doi.org/10.1016/j.ecoenv.2019.109887>.
- [3] P.C. Rúa-Gómez, W. Püttmann, Degradation of lidocaine, tramadol, venlafaxine and the metabolites *O*-desmethyltramadol and *O*-desmethylvenlafaxine in surface waters, *Chemosphere.*, 90 (2013) 1952–1959.
- [4] S. Arriaga, N. de Jonge, M.L. Nielsen, H.R. Andersen, V. Borregaard, K. Jewel, T.A. Ternes, J.L. Nielsen, Evaluation of a membrane bioreactor system as post-treatment in waste water treatment for better removal of micropollutants, *Water Res.*, 107 (2016) 37–46.
- [5] P.C. Rúa-Gómez, W. Püttmann, Occurrence and removal of lidocaine, tramadol, venlafaxine, and their metabolites in German wastewater treatment plants, *Environ. Sci. Pollut. Res.*, 19 (2012) 689–699.
- [6] O. Golovko, V. Kumar, G. Fedorova, T. Randak, R. Grabic, Removal and seasonal variability of selected analgesics/anti-inflammatory, anti-hypertensive/cardiovascular pharmaceuticals and UV filters in wastewater treatment plant, *Environ. Sci. Pollut. Res.*, 21 (2014) 7578–7585.
- [7] V. Calisto, C.I.A. Ferreira, J.A.B.P. Oliveira, M. Otero, V.I. Esteves, Adsorptive removal of pharmaceuticals from water by commercial and waste-based carbons, *J. Environ. Manage.*, 152 (2015) 83–90.
- [8] C. Wahlberg, B. Björleinius, N. Paxéus, Fluxes of 13 selected pharmaceuticals in the water cycle of Stockholm, Sweden, *Water Sci. Technol.*, 63 (2011) 1772–1780.
- [9] J. Vymazal, T. Dvořáková Březinová, M. Koželuh, L. Kule, Occurrence and removal of pharmaceuticals in four full-scale constructed wetlands in the Czech Republic – the first year of monitoring, *Ecol. Eng.*, 98 (2017) 354–364.
- [10] S.C. Monteiro, A.B.A. Boxall, Factors affecting the degradation of pharmaceuticals in agricultural soils, *Environ. Toxicol. Chem.*, 28 (2009) 2546–2554.
- [11] Y. Zhang, H. Zhu, U. Szewzyk, S. Lübbecke, S. Uwe Geissen, Removal of emerging organic contaminants with a pilot-scale biofilter packed with natural manganese oxides, *Chem. Eng. J.*, 317 (2017) 454–460.
- [12] P. Sehonova, Z. Svobodova, P. Dolezelova, P. Vosmerova, C. Faggio, Effects of waterborne antidepressants on non-target animals living in the aquatic environment: a review, *Sci. Total Environ.*, 631–632 (2018) 789–794.
- [13] S. Mompelat, B. Le Bot, O. Thomas, Occurrence and fate of pharmaceutical products and by-products, from resource to drinking water, *Environ. Int.*, 35 (2009) 803–814.

- [14] D. Löffler, J. Römbke, M. Meller, T.A. Ternes, Environmental fate of pharmaceuticals in water/sediment systems, *Environ. Sci. Technol.*, 39 (2005) 5209–5218.
- [15] P.H. Roberts, K.V. Thomas, The occurrence of selected pharmaceuticals in wastewater effluent and surface waters of the lower Tyne catchment, *Sci. Total Environ.*, 356 (2006) 143–153.
- [16] D.W. Kolpin, M. Skopec, M.T. Meyer, E.T. Furlong, S.D. Zaugg, Urban contribution of pharmaceuticals and other organic wastewater contaminants to streams during differing flow conditions, *Sci. Total Environ.*, 328 (2004) 119–130.
- [17] A.C. Hari, R.A. Paruchuri, D.A. Sabatini, T.C.G. Kibbey, Effects of pH and cationic and nonionic surfactants on the adsorption of pharmaceutical to a natural aquifer material, *Environ. Sci. Technol.*, 39 (2005) 2592–2598.
- [18] A.Y. Lin, M. Reinhard, Photodegradation of common environmental pharmaceuticals and estrogens in river water, *Environ. Toxicol. Chem.*, 24 (2005) 1303–1309.
- [19] G. Annadurai, Design of optimum response surface experiments for adsorption of direct dye on chitosan, *Bioprocess Eng.*, 23 (2000) 451–455.
- [20] B. Kasprzyk-Hordern, R.M. Dinsdale, A.J. Guwy, Illicit drugs and pharmaceuticals in the environment – forensic applications of environmental data, Part 2: pharmaceuticals as chemical markers of faecal water contamination, *Environ. Pollut.*, 157 (2009) 1778–1786.
- [21] M. Javanbakht, A.M. Attaran, M.H. Namjumanesh, M. Esfandyari-Manesh, B. Akbari-Adergani, Solid-phase extraction of tramadol from plasma and urine samples using a novel water-compatible molecularly imprinted polymer, *J. Chromatogr. B*, 878 (2010) 1700–1706.
- [22] L.R. Rad, M. Irani, F. Divsar, H. Pourahmad, M.S. Sayyafan, I. Hariirani, Simultaneous degradation of phenol and paracetamol during photo-Fenton process: design and optimization, *J. Taiwan Inst. Chem. Eng.*, 47 (2015) 190–196.
- [23] M.G. Cantwell, D.R. Katz, J.C. Sullivan, D. Shapley, J. Lipscomb, J. Epstein, A.R. Juhl, C. Knudson, G.D. O'Mullan, Spatial patterns of pharmaceuticals and wastewater tracers in the Hudson River Estuary, *Water Res.*, 137 (2018) 335–343.
- [24] M. Rožman, V. Acuña, M. Petrović, Effects of chronic pollution and water flow intermittency on stream biofilms biodegradation capacity, *Environ. Pollut.*, 233 (2018) 1131–1137.
- [25] C. Lütke Eversloh, M. Schulz, M. Wagner, T.A. Ternes, Electrochemical oxidation of tramadol in low-salinity reverse osmosis concentrates using boron-doped diamond anodes, *Water Res.*, 72 (2015) 293–304.
- [26] L. Zhang, X. Yin, S.F.Y. Li, Bio-electrochemical degradation of paracetamol in a microbial fuel cell-Fenton system, *Chem. Eng. J.*, 276 (2015) 185–192.
- [27] U.K. Garg, M.P. Kaur, V.K. Garg, D. Sud, Removal of Nickel(II) from aqueous solution by adsorption on agricultural waste biomass using a response surface methodological approach, *Bioresour. Technol.*, 99 (2008) 1325–1331.
- [28] T. Thiebault, R. Guégan, M. Boussafir, Adsorption mechanisms of emerging micro-pollutants with a clay mineral: case of tramadol and doxepine pharmaceutical products, *J. Colloid Interface Sci.*, 453 (2015) 1–8.
- [29] J.N. Sahu, J. Acharya, B.C. Meikap, Response surface modeling and optimization of chromium(VI) removal from aqueous solution using Tamarind wood activated carbon in batch process, *J. Hazard. Mater.*, 172 (2009) 818–825.
- [30] A. Altinişik, E. Gür, Y. Seki, A natural sorbent, *Luffa cylindrica* for the removal of a model basic dye, *J. Hazard. Mater.*, 179 (2010) 658–664.
- [31] H. Bendjefal, A. Djebli, H. Mamine, T. Metidji, M. Dahak, N. Rebbani, Y. Bouhedja, Effect of the chelating agents on bio-sorption of hexavalent chromium using *Agave sisalana* fibers, *Chin. J. Chem. Eng.*, 26 (2018) 984–992.
- [32] H. Shahbeig, N. Bagheri, S.A. Ghorbanian, A. Hallajisani, S. Poorkarimi, A new adsorption isotherm model of aqueous solutions on granular activated carbon, *World J. Model. Simul.*, 9 (2013) 243–254.
- [33] B. Armagan, F. Toprak, Optimum isotherm parameters for reactive azo dye onto pistachio nut shells: comparison of linear and non-linear methods, *Polish J. Environ. Stud.*, 22 (2013) 1007–1011.
- [34] F.C. Wu, B.L. Liu, K.T. Wu, R.L. Tseng, A new linear form analysis of Redlich–Peterson isotherm equation for the adsorptions of dyes, *Chem. Eng. J.*, 162 (2010) 21–27.
- [35] I. Khalid, S. Ali, M.T. Hussain, R. Ashra, A. Khan, N. Ahmad, investigating the impact of hard water on natural dyeing of cotton fabric by *Tagetes erecta* flowers, *J. Chem. Soc. Pak.*, 41 (2019) 788–795.
- [36] N. Haimour, R. El-Bishtawi, A. Ail-Wahbi, Equilibrium adsorption of hydrogen sulfide onto CuO and ZnO, *Desalination*, 181 (2005) 145–152.
- [37] O. Redlich, D.L. Peterson, A useful adsorption isotherm, *J. Phys. Chem.*, 63 (1959) 1024.
- [38] P.B. Vilela, A. Dalalibera, E.C. Duminelli, V.A. Becegato, A.T. Paulino, Adsorption and removal of chromium (VI) contained in aqueous solutions using a chitosan-based hydrogel, *Environ. Sci. Pollut. Res.*, 26 (2019) 28481–28489.
- [39] M.C. Ncibi, Applicability of some statistical tools to predict optimum adsorption isotherm after linear and non-linear regression analysis, *J. Hazard. Mater.*, 153 (2008) 207–212.
- [40] I. Quesada-Peñate, C. Julcour-Lebigue, U.J. Jáuregui-Haza, A.M. Wilhelm, H. Delmas, Degradation of paracetamol by catalytic wet air oxidation and sequential adsorption – catalytic wet air oxidation on activated carbons, *J. Hazard. Mater.*, 221–222 (2012) 131–138.
- [41] A. Malakahmad, S.Y. Chuan, Application of response surface methodology to optimize coagulation-flocculation treatment of anaerobically digested palm oil mill effluent using alum, *Desal. Water Treat.*, 51 (2013) 6729–6735.
- [42] Q. Chen, Q. Shi, S.N. Gorb, Z.Y. Li, A multiscale study on the structural and mechanical properties of the luffa sponge from *Luffa cylindrica* plant, *J. Biomech.*, 47 (2014) 1332–1339.
- [43] K.S.W. Sing, Reporting physisorption data for gas/solid systems with special reference to the determination of surface area and porosity, *Pure Appl. Chem.*, 54 (1982) 2201–2218.
- [44] M. Thommes, K. Kaneko, A. V. Neimark, J.P. Olivier, F. Rodriguez-Reinoso, J. Rouquerol, K.S.W. Sing, Physisorption of gases, with special reference to the evaluation of surface area and pore size distribution (IUPAC Technical Report), *Pure Appl. Chem.*, 87 (2015) 1051–1069.
- [45] B. Jiang, Z.G. Shen, J.B. Shen, D. Yu, X.Y. Sheng, H.F. Lu, Germination and growth of sponge gourd (*Luffa cylindrica*) pollen tubes and FTIR analysis of the pollen tube wall, *Sci. Hortic. (Amsterdam)*, 122 (2009) 638–644.
- [46] Ç. Sarici-Özdemir, F. Kiliç, Kinetics behavior of methylene blue onto agricultural waste, *Part. Sci. Technol.*, 36 (2018) 194–201.
- [47] D.C.P. Quinayá, J.R.M. D'almeida, Nondestructive characterization of epoxy matrix composites reinforced with luffa lignocellulosic fibers, *Rev. Mater.*, 22 (2017), <https://doi.org/10.1590/s1517-707620170002.0181>.
- [48] Ç. Sarici Özdemir, Adsorptive removal of methylene blue by fruit shell: isotherm studies, *Fullerenes Nanotubes Carbon Nanostruct.*, 26 (2018) 570–577.
- [49] S. Kalia, A. Kumar, B.S. Kaith, Sunn hemp cellulose graft copolymers polyhydroxybutyrate composites: morphological and mechanical studies, *Adv. Mater. Lett.*, 2 (2011) 17–25.
- [50] V. Bernal, A. Erto, L. Giraldo, J.C. Moreno-Piraján, Effect of solution pH on the adsorption of paracetamol on chemically modified activated carbons, *Molecules*, 22 (2017) 1032.
- [51] E.K. Radwan, H.H. Abdel Ghafar, A.S. Moursy, C.H. Langford, A.H. Bedair, G. Achari, Adsorptive removal of hazardous organic water pollutants by humic acid-carbon hybrid materials: kinetics and isotherm study, *Desal. Water Treat.*, 80 (2017) 297–305.
- [52] H.H. Abdel Ghafar, M.A. Embaby, E.K. Radwan, A.M. Abdel-Aty, Biosorptive removal of basic dye methylene blue using raw and CaCl₂ treated biomass of green microalga *scenedesmus obliquus*, *Desal. Water Treat.*, 81 (2017) 274–281.

- [53] S.T. El-Wakeel, E.K. Radwan, H.H. Abdel Ghafar, A.S. Moursy, Humic acid-carbon hybrid material as lead(II) ions adsorbent, *Desal. Water Treat.*, 74 (2017) 216–223.
- [54] H. Demir, A. Top, D. Balköse, S. Ülkü, Dye adsorption behavior of *Luffa cylindrica* fibers, *J. Hazard. Mater.*, 153 (2008) 389–394.
- [55] S.Y. Lagergren, Zur theorie der sogenannten adsorption gelöster stoffe, 1898.
- [56] G. Blanchard, M. Maunaye, G. Martin, Removal of heavy metals from waters by means of natural zeolites, *Water Res.*, 18 (1984) 1501–1507.
- [57] B. Weber, E. Kaps, J. Obel, W. Bauer, Synthesis and magnetic properties of new octahedral iron(II) complexes, *Z. Anorg. Allg. Chem.*, 634 (2008) 1421–1426.
- [58] N. Sonetaka, H.-J. Fan, S. Kobayashi, H.-N. Chang, E. Furuya, Simultaneous determination of intraparticle diffusivity and liquid film mass transfer coefficient from a single-component adsorption uptake curve, *J. Hazard. Mater.*, 164 (2009) 1447–1451.
- [59] F. Rouquerol, J. Rouquerol, K.S.W. Sing, P. Llewellyn, G. Maurin, *Adsorption by Powders and Porous Solids*, Academic Press, London, 2014.

Supplementary information

Table S1

Physicochemical properties of dextropropoxyphene and paracetamol

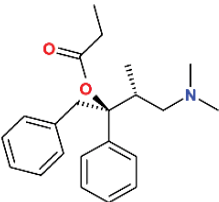
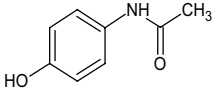
	Structure	M_w (g/L)	pKa	S_w (g/L)	$\log K_{ow}$
Dextropropoxyphene, $C_{22}H_{29}NO_2$, DPP		339.47	6.30	3.32 (25°C)	4.18
Paracetamol, $C_8H_9NO_2$, PAR		151.16	9.50	14 (22°C)	0.46– 0.5

Table S2

Analysis of variance for dextropropoxyphene and paracetamol sorption process

		DF	Sum of squares	Mean square	F-value	p-value
Dextropropoxyphene	Model	1	0.8588	0.8588	99.1702	5.7114×10^{-4}
	Error	4	0.0346	0.0087		
	Total	5	0.8934			
Paracetamol	Model	1	0.5573	0.5573	104.6546	1.8411×10^{-5}
	Error	7	0.0373	0.0053		
	Total	8	0.5946			

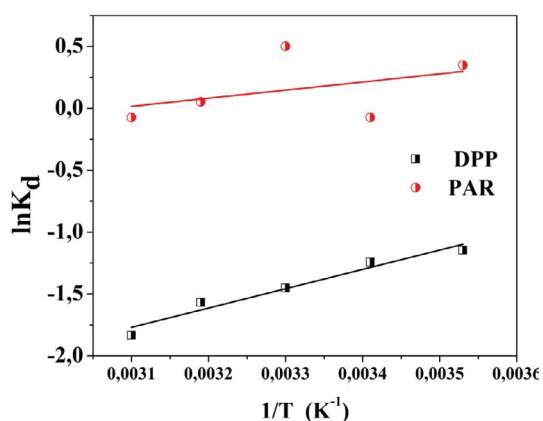


Fig. S1. Thermodynamic parameters for dextropropoxyphene and paracetamol adsorption on *Luffa cylindrica* at different temperatures.